

# Spörer's Law and Relationship between the Latitude and Amplitude Parameters of Solar Activity

V. G. Ivanov and E. V. Miletsky

*Main (Pulkovo) Astronomical Observatory, Russian Academy of Sciences, St. Petersburg, Russia*

*e-mail: vg.ivanov@gao.spb.ru*

Received April 24, 2014

**Abstract**—The equatorward drift of average sunspot latitudes (Spörer's law) and its relationship with other characteristics of the 11-year solar cycle are analyzed. The notion of *cycle latitude phase* (CLP) is introduced, which is calculated from behavior of average sunspot latitudes. The latter are shown to be expressed, with known accuracy, as a universal monotonic decreasing function of the CLP and to be independent of the cycle strength. The same applies to the latitudinal drift velocity of the sunspot generating zone. The shifts in the CLP reference times relative to the cycle minima are, on the contrary, well correlated with the amplitudes of the corresponding cycles. Solar activity in the declining phase of the solar cycle is found to be tightly related to the average sunspot latitude and CLP. The relationships found in the study can be used to reconstruct average sunspot latitudes in the pre-Greenwich epoch based on the available information on cycle amplitudes.

**DOI:** 10.1134/S0016793214070044

## 1. INTRODUCTION

Traditionally, researchers single out certain “reference points” in the development of the 11-year cycle of solar activity. The general tendency is to use for these moments solar activity extrema, which are found from smoothed Wolf numbers or other activity indices, e.g., the areas or amounts of sunspot groups; the times of the extrema may differ slightly in different indices (Hathaway, 2010).

Solar minima are commonly used as reference points to measure the phase of a given 11-year cycle and to study the phase dependences of the various cycle parameters. One of these parameters, the evolution of which throughout the cycle is of interest to researchers, is the average sunspot latitude (ASL).

It is well known that the behavior of sunspot latitudes during the 11-year cycle is described by Spörer's law: the first sunspot groups are formed at high heliolatitudes, and then the center of activity gradually shifts toward the equator (Carrington, 1858; Spörer, 1880; Hathaway et al., 2003).

Sokoloff and Khlystova (2010) showed that the Sun's toroidal magnetic field, which plays an important role in the work of the solar dynamo, has a very simple structure, which is visualized without major distortion in the latitude–time distribution of sunspot known as Maunder's butterfly diagram. This opens up the possibility to test various dynamo models by analyzing their consistency with the observed features of the latitudinal and temporal evolution of sunspots throughout the 11-year cycle (e.g., the change in the shape and size of the butterfly wings, the pattern of the equatorward sunspot drift, etc.).

It has long been observed that ASL behavior changes less from cycle to cycle than the amplitude parameters of solar activity. The fact that the drift described by Spörer's law is almost independent of the cycle number has been reported, e.g., in (Eigenson et al., 1948; Vitinskii, Kopetskii, and Kuklin, 1986). A similar conclusion was made by Hathaway (2011), who showed that cycle starting times ( $T_{\text{cst}}$ ) can be shifted relative to their minima so that the ASL behavior would be universally dependent on the time that passed since  $T_{\text{cst}}$ .

The times  $T_{\text{cst}}$  were calculated in (Hathaway, 1994) based on the behavior of the Wolf numbers near the 11-year cycle minima. However, it would be interesting to obtain moments with similar properties without relying on solar cycle amplitudes. In this work we present one of the ways to do it, using the ASL data only. We also discuss the relationships of the resulting moments with solar cycle amplitudes.

## 2. DATA AND METHOD

The source of data on sunspot latitudes was the extended Greenwich catalog, which includes the original Greenwich data and their continuation by NOAA/USAF (<http://solarscience.msfc.nasa.gov/greenwch.shtml>) and contains the coordinates and areas of sunspot groups for the period 1874–2013.

It is known that sunspot groups corresponding to different wings in the butterfly diagram (thus, to different cycles) may coexist in the neighborhood of cycle minima. Taking this fact into consideration, we divided the sunspot groups in each hemisphere into

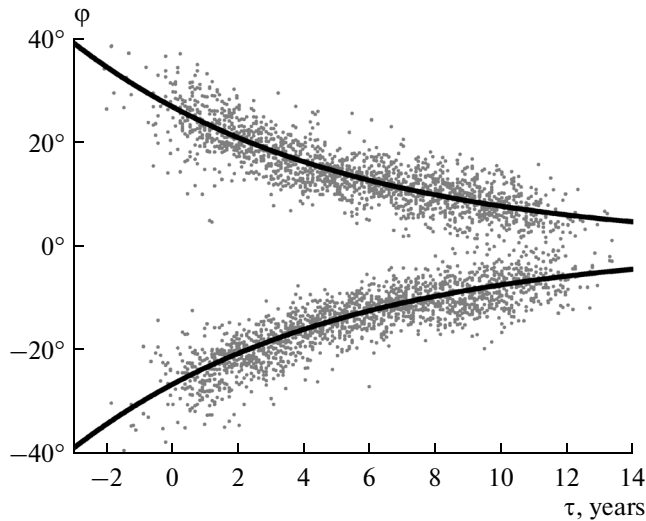


**Fig. 1.** Rotation-average sunspot latitudes (dots) and their approximation by the functions  $\pm\Psi(\tau; a_0, b_0)$ .

two subsets corresponding to the upper and lower butterfly wings (the technique used to make this division was described in detail in (Ivanov et al., 2011)).

Using the catalog data, we calculated for a given hemisphere and wing the daily numbers  $G$  of sunspot groups and their average latitudes  $\phi$  weighted by sunspot areas. The resulting  $G$  and  $\phi$  were averaged over the solar rotations. Taking into account the above division, we obtained for each rotation from two (if the butterfly wings did not overlap at all) to four (if the wings overlapped in both hemispheres) values of the “partial”  $G$  index. In this case, as is shown in (Ivanov and Miletsky, 2011), the total  $G$  index for the disk (*sunspot number index*), after appropriate renormalization, is very close to the GSN index proposed by Hoyt and Schatten (1998).

Below we also use the times of the extrema  $T_{\min}$  and  $T_{\max}$  of the solar cycles. They were calculated using the  $G$  index smoothed with a 13-point sinusoidal filter (SIN13), which was determined by the weights

$$w_j = \cos(j\pi/14), \quad j = -6, \dots, 6.$$

These times of minima in  $G$  are close to the minima in the Wolf numbers  $T_{\min, W}$  smoothed using the same filter: the mean square difference between the times of minima in these two indices for cycles 12–23 is approximately 0.14 yr.

### 3. CYCLE LATITUDE PHASES

We now consider a series of rotation averages  $\phi_i(\tau)$  depending the *cycle amplitude phase*  $\tau = t - T_{\min, i}$ , where  $t$  is time and  $T_{\min, i}$  are the times of minima in the smoothed  $G$  index for a given cycle and hemisphere. Here the  $i$  index labels either the cycle number only or,

if we are working with hemisphere indices, the cycle and the hemisphere.

Figure 1 shows the rotation averages  $\phi_i$  for all the cycles and hemisphere as a function of  $\tau$ . We seek to approximate the resulting dependence by exponential functions

$$\Psi(\tau, a, b) = \pm a \exp(b\tau),$$

where  $a$  and  $b$  are free parameters for which the weighted least squares method (with weights  $G$ ) yields  $a = 26.6 \pm 0.2^\circ$  and  $b = -0.126 \pm 0.002 \text{ yr}^{-1}$ . The first parameter indicates the reference latitude at which the exponential curve crosses the  $Y$ -axis; the second stands for the velocity of the equatorward drift of the sunspot latitudes. Very similar values for the coefficients ( $a = 26.8^\circ \pm 0.3^\circ$  and  $b = -0.125 \pm 0.003 \text{ yr}^{-1}$ ) were obtained in (Ivanov and Miletsky, 2013), which used the same data but no division by butterfly wings and made approximations only for a portion of the dependence in the phase range  $2 \leq \tau \leq 8 \text{ yr}$ . The approximating curves  $\pm\Psi(\tau; a_0, b_0)$  are depicted in Fig. 1. The RMS error of the approximation is  $2.5^\circ$  (the correlation coefficient  $R = 0.96$ ).

Similar exponential functions were used to describe the average latitude by Hathaway (2011) and Roshchina and Sarychev (2011), who obtained similar values for the  $b$  parameter:  $-0.1237 \text{ yr}^{-1}$  (Roshchina and Sarychev, 2011) and  $-1/90 \text{ mo}^{-1} \approx -0.13 \text{ yr}^{-1}$  (Hathaway, 2011).

The resulting total curve can be used to describe ASL behavior in individual cycles. We approximate  $\phi_i(\tau)$  by the functions  $\Psi(\tau; a_0, b_0)$ , where the general parameter  $b_0$  was found above and  $a_i$  is fitted for each cycle and hemisphere  $i$ . These functions can be put in a general form

$$\Psi(\tau, a_i, b_0) = \Psi(\tau - \Delta T_i; a_0, b_0),$$

where  $\Delta T_i = 1/b_0 \log(a_0/a_i)$  are shifts of the individual curve, which are found so as to minimize the mean square difference between the approximating function and  $\phi_i(\tau)$  for a given  $i$ .

The search for an optimal shift  $\Delta T$  is illustrated in Fig. 2 by the example of the northern hemisphere in cycle 19; the smoothed average latitudes and the resulting approximating curves for all cycles are shown in Fig. 3.

The same procedure can be used to find the shifts  $\Delta T_i$  for ASLs without the division by hemisphere. In this case the absolute ASL values are averaged over the entire disk and the  $i$  index labels the cycle number only. The resulting times  $T_0 = T_{\min} + \Delta T$  for the separate hemispheres and whole disk are given in Table 1. The table also cites the times of minima  $T_{\min}$  and maxima  $T_{\max}$  and the maximum values of the SIN13-smoothed  $G$  index.

Apparently,  $T_i$  indicate the times at which the latitude of the individual approximating curves reaches

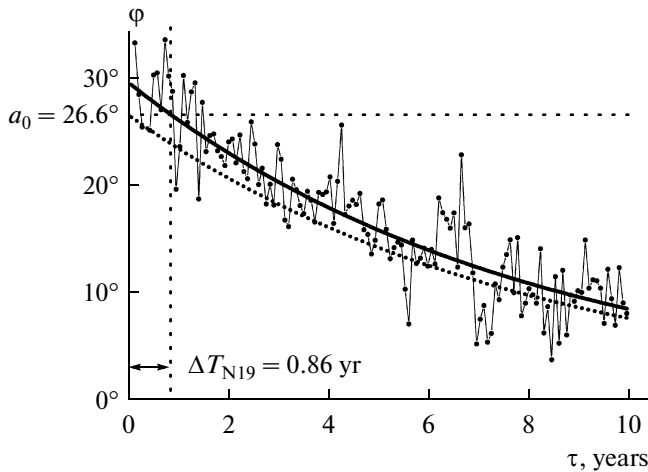


**Fig. 2.** Search for an optimal shift illustrated by the example of the northern hemisphere in cycle 19. The thin curve shows the rotation average sunspot latitudes; the dotted line is  $\Psi(\tau; a_0, b_0)$ ; and the thick solid line is  $\Psi(\tau; a_{N19}, b_0)$ .

the reference value  $\Psi(\Delta T_i; a_i, b_0) = \Psi(0; a_0, b_0) = a_0 = 26.6^\circ$  (Fig. 2).

It should be noted that, generally speaking, we could use an individual parameter  $b_i$  for each cycle and hemisphere. However, as shown by our calculations, the resulting decrease in the approximation errors is small (on average, a few percent); hence, we can use the general parameter  $b_0$  for all cycles without compromising the quality of the ASL approximation.

The times  $T_0$  can be used to calculate the phase of the 11-year cycle in the same way as the times of minima  $T_{\min}$ . To emphasize the difference between the two definitions of the phase, we refer to  $\tau = t - T_{\min}$  as the *cycle amplitude phase* (CAP) and to  $\chi = t - T_0$  as the *cycle latitude phase* (CLP). Consequently, it is natural to call  $T_0$  the *latitude phase reference points* (LPRPs).

Since in each cycle and hemisphere the characteristic latitude of the approximating curve  $\psi = \Psi(\chi; a_0, b_0)$  corresponds to the same  $\chi$ , the value  $\psi$  also can be used as measure of ASL.

Since the LPRPs were found under the assumption that the drift of the sunspot zones in the 11-year cycle (Spörer's law) is universal, they are close, as expected, to the cycle starting times  $T_{\text{cst}}$  found by Hathaway (2011). It should be noted, however, that the  $T_{\text{cst}}$  were found by analyzing the behavior of the Wolf numbers near the 11-year cycle minimum, whereas the only source of data to calculate  $T_0$  were the sunspot latitudes.

In addition, it should be noted that we can choose any other baseline latitude instead of  $a_0 = 26.6^\circ$ . This would result in a general shift of all  $T_0$ ; however, it would not affect the properties that are discussed below. Therefore, it would be incorrect to consider the LPRPs as the 11-year cycle starting times. In this way they differ from the cycle starting times in (Hathaway, 2011), which are, in a sense, the times at which the activity in the cycle begins.

#### 4. PROPERTIES OF THE LATITUDINAL PHASE REFERENCE POINTS

Figure 4 shows the shifts of the LPRPs relative to the cycle minima  $T_{\min}$  for the two hemispheres and whole disk as a function of the cycle number. There is a noticeable secular trend: the shifts in cycles 12–21 increase with the cycle number. A similar yet less pronounced trend can be seen in the shifts  $T_{\text{cst}} - T_{\min}$ .

This trend can be explained by the joint action of two factors: the rising phase of the secular cycle during the first two thirds of the 20th century and the correlation between  $\Delta T$  and cycle amplitude. In fact the correlation coefficient between  $\Delta T$  and the sunspot group index at the cycle maxima  $G_{\text{max}}$  is +0.74 (for the whole

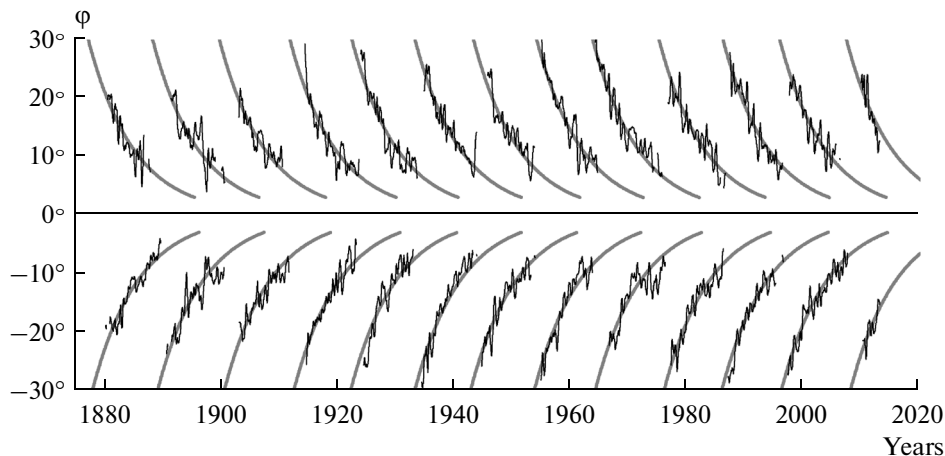


**Fig. 3.** Smoothed average sunspot latitudes and the approximating curves  $\Psi(\tau; a_i, b_0)$ .

**Table 1.** Solar cycle extrema for the G index and  $T_0$ 

Cycle	Northern hemisphere				Southern hemisphere				Whole disk			
	$T_{\min}$	$T_0$	$T_{\max}$	$G_{\max}$	$T_{\min}$	$T_0$	$T_{\max}$	$G_{\max}$	$T_{\min}$	$T_0$	$T_{\max}$	$G_{\max}$
12	1879.1	1877.9	1881.8	2.84	1878.6	1878.6	1884.1	4.09	1879.0	1878.3	1884.1	6.76
13	1889.5	1889.0	1894.4	3.65	1890.1	1889.9	1893.5	5.20	1890.1	1889.4	1893.6	8.84
14	1901.9	1900.5	1906.2	3.70	1901.3	1901.3	1908.3	3.08	1901.4	1900.8	1906.2	5.61
15	1912.5	1912.6	1917.6	5.43	1913.5	1913.3	1917.7	4.58	1913.5	1912.7	1917.7	9.99
16	1923.9	1923.3	1929.8	3.85	1923.3	1923.0	1927.3	4.15	1923.3	1923.0	1928.4	7.43
17	1933.9	1934.1	1937.4	6.21	1933.3	1934.1	1938.4	4.98	1933.7	1934.0	1937.4	10.69
18	1944.4	1944.2	1949.9	6.02	1944.1	1943.7	1947.5	6.56	1944.2	1944.0	1947.6	12.36
19	1954.2	1955.0	1959.3	9.14	1954.3	1954.6	1957.8	7.23	1954.3	1954.9	1958.0	15.05
20	1964.6	1964.7	1967.3	5.78	1964.9	1965.1	1970.2	5.07	1964.6	1964.7	1970.3	9.54
21	1976.2	1976.1	1979.5	8.10	1975.2	1976.9	1979.1	6.93	1976.1	1976.4	1979.5	14.57
22	1986.0	1987.1	1989.7	7.33	1986.4	1986.9	1991.4	8.12	1986.3	1987.1	1989.7	13.58
23	1996.8	1996.8	2001.7	5.29	1996.4	1997.1	2002.4	5.53	1996.5	1996.9	2002.1	10.36

disk) and  $+0.61$  (for separate hemispheres) (Table 2 and Fig. 5). The plus sign of the correlation coefficient indicates that  $T_0$  is behind the cycle minima in high cycles and ahead of them in low cycles. This means, in turn, that for a given  $\tau$  (i.e., time measured from the cycle minimum), sunspot groups in high cycles are, as a rule, located higher.

The use of LPRPs may strengthen the well-known inverse correlation between the length of the rising phase  $T_{\text{inc}} = T_{\text{max}} - T_{\text{min}}$  and the amplitude of the 11-year cycle (Waldmeier's rule). The correlation is typ-

ically calculated using the Wolf numbers; the corresponding coefficient for cycles 12–23 (the epoch of the extended Greenwich catalog) is  $R = -0.65$ . The correlation coefficient for G is slightly lower,  $R = -0.63$ , if the index is taken for the whole disk and falls to  $R = -0.25$  when calculated for the separate hemispheres. However, if we modify Waldmeier's rule by taking the intervals  $T_{0,\text{inc}} = T_{\text{max}} - T_0$  as the lengths of the rising phases, the correlations for G increase to  $R = -0.83$  (whole disk) and  $R = -0.56$  (separate hemispheres) (Table 2).

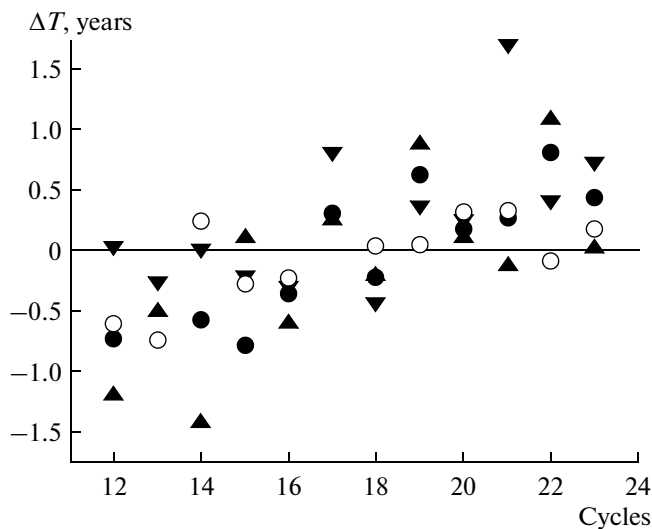


**Fig. 4.** Shifts of  $T_0$  relative to the cycle minima  $T_{\min}$  for the northern (upward pointing triangles) and southern (downward pointing triangles) hemispheres and for the whole disk (solid circle symbols). The open circle symbols indicate the shifts of the times  $T_{\text{cst}}$  (Hathaway, 2011).

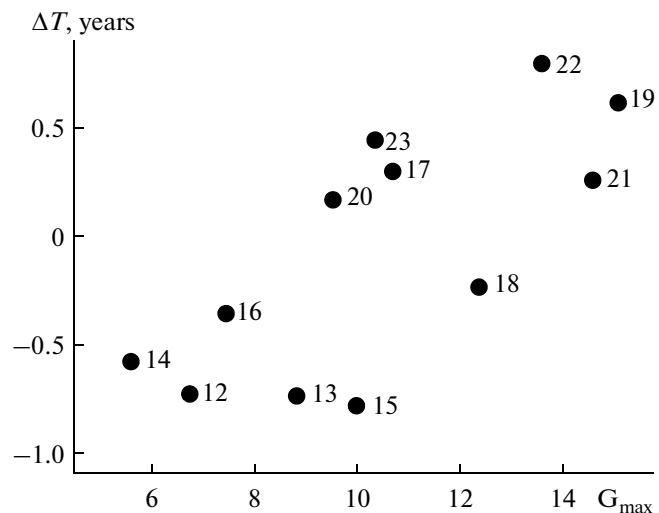


**Fig. 5.** Relationship between the cycle amplitude ( $G_{\max}$ ) and the shift of  $T_0$  relative to the cycle minima ( $\Delta T$ ) for the whole disk. The numbers in plot indicate solar cycle numbers.

It should be noted that the behavior of the solar activity indices in the 11-year cycle looks different when the cycle phase is described by different variables. Figure 6a shows the behavior of  $G(\tau)$  (two hemispheres; cycles 12–23) as a function of the CAP. It is evident that the dispersion of individual curves in the rising phase is approximately the same as in the declining phase (Fig. 6c). In Fig. 6b  $G(\psi)$  is plotted as a function of the CLP. In this case the situation is different: the dispersion is evidently lower in the rising phase. A similar situation is observed for the Wolf numbers (Fig. 6d). The latter fact was noted already by Gnevyshev and Gnevysheva (1949), who showed that the Wolf number in the declining phase depends on the average sunspot latitudes.

It can be shown that for  $\psi < 12^\circ$  this dependence could be quite accurately (with an RMS error of approximately 0.4 units) described by the relationship

$$G(\psi) = 0.061\psi^2 - 0.557\psi + 1.228. \quad (1)$$

**Table 2.** Correlation coefficients  $R$  and confidence levels  $CL$  for the relationships between the amplitudes and the differences between the various reference points in solar cycle for the separate hemispheres (N&S) and whole disk (Disk)

	N&S		Disk	
	$R$	$CL$	$R$	$CL$
$R(G_{\max}, \Delta T)$	+0.61	0.999	+0.74	0.994
$R(W_{\max}, T_{\text{inc}, W})$			−0.65	0.98
$R(G_{\max}, T_{\text{inc}})$	−0.25	0.75	−0.63	0.97
$R(G_{\max}, T_{0, \text{inc}})$	−0.56	0.996	−0.86	0.9997

The corresponding equation for  $W$  (with an error of approximately 8 units) is

$$W(\psi) = 1.181\psi^2 - 9.224\psi + 14.263. \quad (2)$$

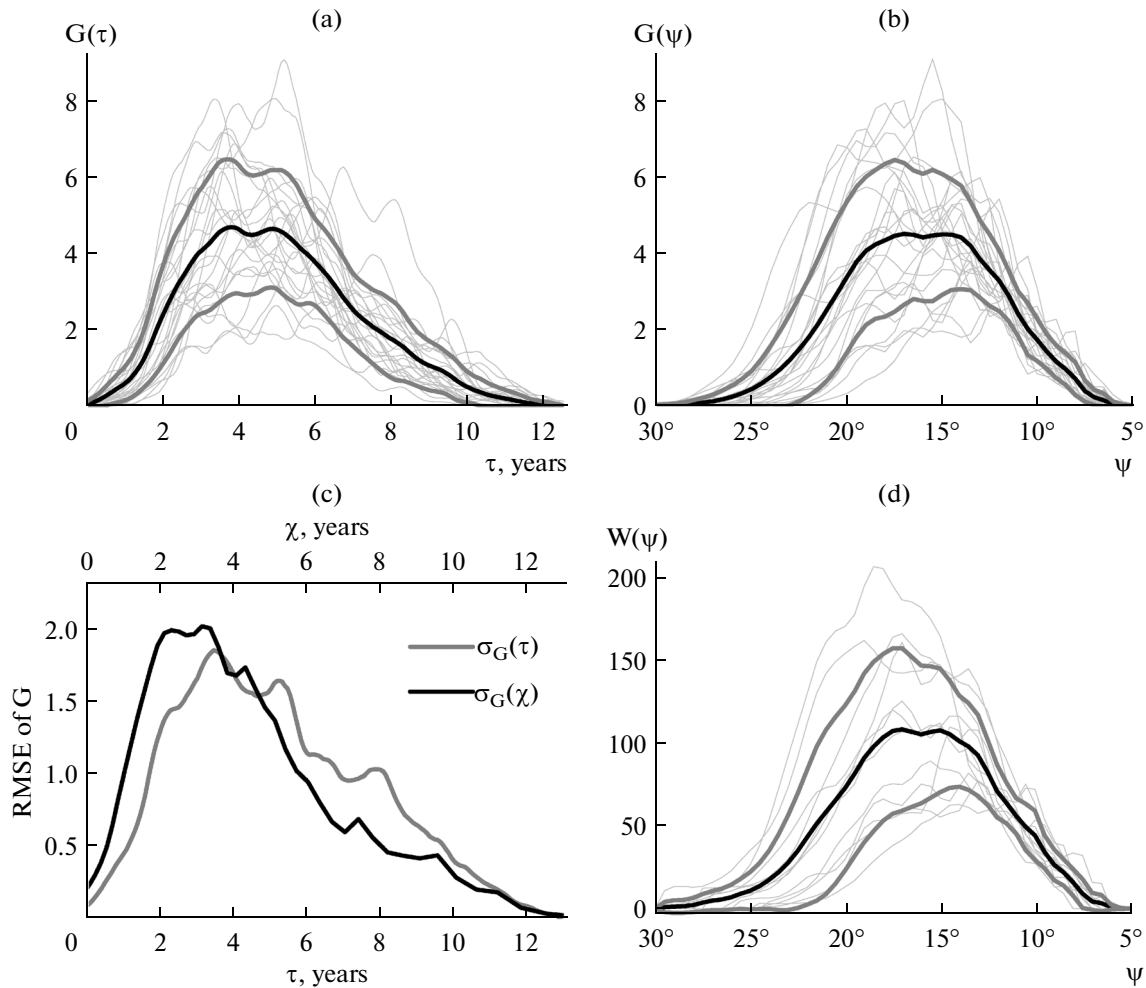


**Fig. 6.** Dependence of the  $G$  and  $W$  indices on the cycle phase for different definitions of the latter: (a)  $G(\tau)$ ; (b)  $G(\psi)$ ; (c) RMS deviations  $\sigma_G(\tau)$  and  $\sigma_G(\chi)$  of individual curves relative to the average curve for the  $G$  index for different phase definitions; and (d)  $W(\psi)$ .

**Table 3.** Reconstruction of LPRPs  $T_{0,W}$  from the Wolf numbers for cycles 1–23 and comparison with the exact times  $T_0$  for cycles 12–23

Cycle	$T_{0,W}$	$T_0$	$\Delta T$	$\Delta T$	Cycle	$T_{0,W}$	$T_0$	$\Delta T$	$\Delta T$
1	1756.2		0.9		13	1889.0	1889.4	−1.1	−0.7
2	1765.8		−0.8		14	1901.4	1900.8	−0.3	−0.6
3	1774.7		−0.7		15	1912.7	1912.7	−0.7	−0.8
4	1786.4		2.0		16	1922.6	1923.0	−0.7	−0.4
5	1798.0		−0.4		17	1934.1	1934.0	0.4	0.3
6	1809.9		−0.7		18	1944.5	1944.0	0.2	−0.2
7	1824.0		0.6		19	1954.6	1954.9	0.4	0.6
8	1833.7		0.1		20	1965.9	1964.7	1.3	0.2
9	1845.5		2.0		21	1976.9	1976.4	0.7	0.3
10	1856.6		0.6		22	1986.4	1987.1	−0.4	0.8
11	1866.8		−0.4		23	1996.9	1996.9	0.5	0.4
12	1877.9	1878.3	−1.0	−0.7					

## 5. ESTIMATES FOR THE AVERAGE SUNSPOT LATITUDE FROM THE AMPLITUDE INDICES

To reconstruct the spatial patterns of solar activity in the past, it is important to have ASL estimates for the times preceding the Greenwich catalog (Nagovitsyn et al., 2010). These estimates could use Eq. (2), which relates ASLs with the Wolf number. Indeed, if we know the behavior of  $W$  in the declining phase, we can find the value of  $T_{0,W}$  at which the function  $W(\Psi(t - T_{0,W}; a_0, b_0))$  best approximates the observed values of  $W$  over the phase range  $\psi < 12^\circ$ .

We consider  $T_{0,W}$  as an estimate for  $T_0$ . To control the accuracy of the estimate, we compared  $T_{0,W}$  and  $T_0$  over the entire range (cycles 12–23; Table 3). The difference between these times is substantial (the RMS error is roughly 0.5 yr); however, the shifts  $\Delta T = T_0 - T_{\min}$  and  $\Delta T_W = T_{0,W} - T_{\min,W}$  have the same sign in 10 cases out of 12, and the correlation between the shifts is rather high ( $R = 0.67$ ), which means that the reconstruction is qualitatively correct.

The resulting  $T_{0,W}$  allow us to build a series of curves  $\Psi(t - T_{0,W}; a_0, b_0)$ , which can be considered as ASL estimates.

Figure 7 shows an ASL reconstruction made by the above method using a monthly series of Wolf numbers since 1749. It is evident that the reconstructed values (thick gray curves) are well consistent with the actual latitudes in the Greenwich epoch (thin black curve). The estimates for the earlier times are also consistent with the average latitudes in the compilation of early observations in the ESAI database (Nagovitsyn et al., 2004) and Schwabe's observations (Arlt et al., 2013); in the latter case, a small systematic deviation is observed for cycle 9 only. The mean error of the ASL estimate based on the reconstructed approximating

curves is only 10% larger than that of the estimate made using the curves built from the exact LPRPs.

## 6. CONCLUSIONS

In this work we introduced a new type of reference moments describing the development of the 11-year solar cycle, i.e., the latitude phase reference points (LPRPs)  $T_0$ .

These times have a number of remarkable properties that distinguish them from cycle minima, which are traditionally used as points from which the phase is measured. First of all, the calculation of LPRPs is based on the information about the average sunspot latitudes rather than amplitude indexes.

The use of  $T_0$  makes it possible to define the cycle latitude phase in a given cycle and hemisphere  $\chi = t - T_0$ . The average sunspot latitude is approximately (RMSE  $\approx 2.5^\circ$  for rotation averages) described by a universal monotonically decreasing function of  $\chi$ :

$$\psi(\chi) = a_0 \exp(b_0 \chi),$$

where the coefficients  $a_0 = 26.6^\circ \pm 0.2^\circ$  and  $b_0 = -0.126^\circ \pm 0.002 \text{ yr}^{-1}$  do not depend on the cycle amplitude. When the cycle phase is defined as the time that has passed since the cycle minimum and is described by the variable  $\tau = t - T_{\min}$ , no such universality is observed, and the average latitudes can be described by the function

$$\psi(t) = a_i \exp(b_0 \tau),$$

where  $a_i$  tends to be larger for high cycles. Nevertheless, the  $b_0$  coefficient remains universal. This means that the velocity of the equatorward drift shows no notable dependence on the amplitude of the 11-year

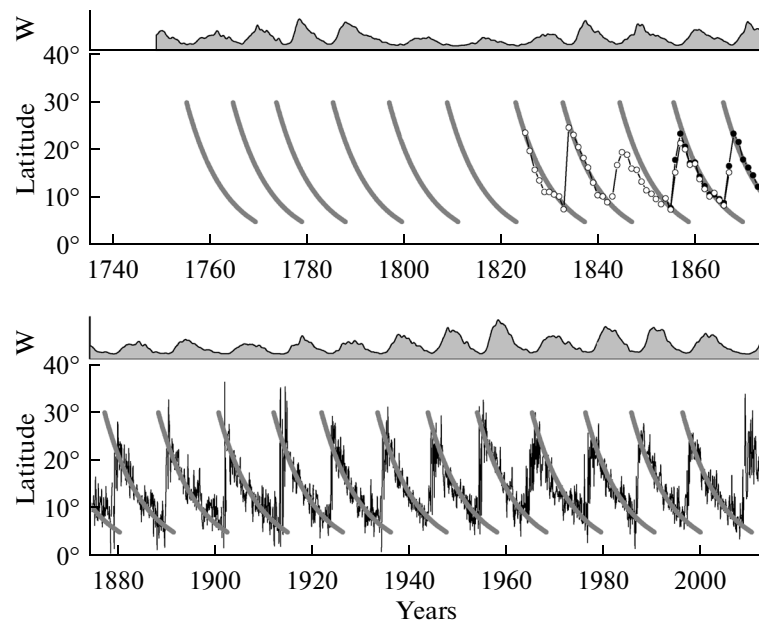


**Fig. 7.** Reconstruction of average sunspot latitudes from the Wolf numbers. The thin black lines are the observed rotation-average latitudes from the data of the extended Greenwich catalog; the thick gray curves are the reconstructions. The figure also shows annual average latitudes in the pre-Greenwich epoch from the ESAI data (Nagovitsyn et al., 2004) (solid circle symbols) and Schwabe's observations (Arlt et al., 2013) (open circle symbols). The curves with gray shading in the individual panels are the smoothed Wolf numbers.

cycle, which confirms the conclusions made in (Hathaway, 2011; Roshchina and Sarychev, 2011).

The difference between the two reference times  $\Delta T = T_0 - T_{\min}$  also increases with the increase in the cycle amplitude (Fig. 5). Consequently, Waldmeier's rule (rather its analogue) is more pronounced, especially in the G index, if we consider the times  $T_0$ , not  $T_{\min}$ , as the reference points of the cycle phase.

We emphasize that the relationship between the cycle amplitude, the time of minimum, and the behavior of average sunspot latitudes reflects the dependence between two types of solar activity characteristics. The characteristics of the first type (cycle amplitudes and the times of minima and maxima) are calculated using the cycle strength parameters, and those of the second type are based on the spatial distribution of activity across the disk. The form of the relationship between the two types of parameters is a priori not obvious. The well-known Spörer's law, in its traditional formulation, is a qualitative statement about sunspot latitudes having a tendency to decrease over the cycle. In our paper we showed that, first, the average sunspot latitude curve is, with known accuracy, universal, provided that the cycle phase is measured from the time  $T_0$ , and, second, the shifts in said curve relative to the cycle minimum  $T_0 - T_{\min}$  depend on the cycle amplitude. Thus, we propose a quantitative relationship between the spatial and power characteristics of the cycle.

In addition to the aforementioned, the universal nature of the latitudinal drift law is manifest in the fact

that the level of activity in the descending phase of the cycle is quite closely related to the CLP and, thus, with sunspot latitudes. This relationship enables us to reconstruct the behavior of the average latitude from the amplitude indices, e.g., the Wolf numbers (as shown above) or GSN index, which is also known for the pre-Greenwich epoch.

The regularities in the latitudinal sunspot distribution and its development over the 11-year cycle impose certain patterns on the possible mechanisms of the solar cycle. The fact that the equatorward drift velocity of the sunspot zones is independent of the cycle amplitude speaks in favor of the dynamo models that do not use the meridional circulation effect (Pipin, Sokoloff, and Usoskin, 2012). The fact that LPRPs tend to lag relative to minima of strong cycles and be ahead of minima of weak cycles could be another argument in favor of theoretical models that can explain this regularity. Finally, the tight relationship between the average sunspot latitude and the level of activity in the descending branch of the cycle may be a consequence of the change in magnetic field generation and should also be taken into account in realistic models of the solar cycle.

#### ACKNOWLEDGMENTS

This work was supported by the Russian Foundation for Basic Research, project no. 13-02-00277; by the Presidential Program for the Support of Leading Science Schools, project no. NSh-1625.2012.2; and

by the Presidium of the Russian Academy of Sciences, programs no. 21 and 22.

## REFERENCES

- Arlt, R., Leussu, R., Giese, N., Mursula, K., and Usoskin, I.G., Sunspot positions and sizes for 1825–1867 from the observations by Samuel Heinrich Schwabe, *Mon. Not. Roy. Astron. Soc.*, 2013, vol. 433, pp. 3165–3172.
- Carrington, R.C., On the distribution of the solar spots in latitudes since the beginning of the year 1854, with a map, *Mon. Not. Roy. Astron. Soc.*, 1858, vol. 19, pp. 1–3.
- Eigenson, M.S., Gnevyshev, M.N., Ol', A.I., and Rubashev, B.M., *Solnechnaya aktivnost' i ee zemnye proyavleniya* (Solar Activity and Its Terrestrial Manifestations), Moscow: Gostekhizdat, 1948.
- Gnevyshev, M.N. and Gnevysheva, R.S., Link between Schwabe–Wolf and Spörer laws, *Byull. Komiss. Issl. Solntsa*, 1949, no. 1(15), pp. 1–8.
- Hathaway, D.H., Wilson, R.M., and Reichmann, R.J., The shape of the sunspot cycle, *Sol. Phys.*, 1994, vol. 151, pp. 177–190.
- Hathaway, D.H., Nandy, D., Wilson, R.M., and Reichmann, R.J., Evidence that a deep meridional flow sets the sunspot cycle period, *Astrophys. J.*, 2003, vol. 589, pp. 665–670.
- Hathaway, D.H., *Liv. Rev. Sol. Phys.*, 2010, vol. 7, no. 1.
- Hathaway, D.H., A standard law for the equatorward drift of the sunspot zones, *Sol. Phys.*, 2011, vol. 273, pp. 221–230.
- Hoyt, D.V. and Schatten, K.H., Group sunspot numbers: a new solar activity reconstruction, *Sol. Phys.*, 1998, vol. 179, pp. 189–219.
- Ivanov, V.G. and Miletsky, E.V., Width of sunspot generating zone and reconstruction of butterfly diagram, *Sol. Phys.*, 2011, vol. 268, pp. 231–242.
- Ivanov, V.G., Miletsky, E.V., and Nagovotsyn Yu.A., Form of the latitude distribution of sunspot activity, *Astron. Rep.*, 2011, vol. 55, no. 10, pp. 911–917.
- Ivanov, V.G. and Miletsky, E.V., Abstracts of Papers, *Trudy vserossiiskoi konferentsii "Solnechnaya i solnechno-zemnaya fizika-2012"* (Proc. All-Russian Conf. on Solar and Solar–Terrestrial Physics, 2012), St. Petersburg, 2012, pp. 51–54.
- Nagovitsyn, Yu.A., Ivanov, V.G., Miletsky, E.V., and Volobuev, D.M., ESAI database and some properties of solar activity in the past, *Sol. Phys.*, 2004, vol. 224, pp. 103–112.
- Nagovitsyn, Yu.A., Ivanov, V.G., Miletsky, E.V., and Nagovitsyna, E.Yu., The Maunder minimum: North-south asymmetry in sunspot formation, mean sunspot latitudes, and the butterfly diagram, *Astron. Rep.*, 2010, vol. 54, no. 5, pp. 476–480.
- Pipin, V.V., Sokoloff, D.D., and Usoskin, I.G., *Astron. Astrophys.*, 2012, vol. 542. Article ID A26.
- Roshchina, E.M. and Sarychev, A.P., Spörer's law and the rhythm of sunspot cycles, *Sol. Syst. Res.*, 2011, vol. 45, pp. 365–371.
- Sokoloff, D. and Khlystova, A.I., The solar dynamo in the light of the distribution of various sunspot magnetic classes over butterfly diagram, *Astron. Nachr.*, 2010, vol. 331, p. 82.
- Spörer, G., Beobachtungen der Sonnenflecken von Januar 1874 bis December 1879, *Publ. Astrophys. Potsdam*, 1880, vol. 2, p. 1.
- Vitinskii, Yu.I., Kopetskii, M., and Kuklin, G.V., *Statistika pyatnoobrazovatel'noi deyatel'nosti Solntsa* (Statistics of the Spot-Forming Activity of the Sun), Moscow: Nauka, 1986.

*Translated by A. Kobkova*